

Phase Equilibrium in Carbothermal Reduction $\text{Al}_2\text{O}_3 \rightarrow \text{AlN}$ Studied by Thermodynamic Calculations

Chien Chon Chen¹, Chih Yuan Chen¹, Hsi Wen Yang², Yang Kuao Kuo³, and Jin Shyong Lin^{4,*}

¹ Department of Energy Engineering, National United University, Miaoli 36003, Taiwan; ² Department of Materials Science and Engineering, National United University, Miaoli 36003, Taiwan; ³ Chung-Shan Institute of Science and Technology, Taoyuan 325, Taiwan; ⁴ Department of Mechanical Engineering, National Chin-Yi University of Technology, Taichung 411, Taiwan.

Received: July 16, 2014 / Accepted: August 22, 2014

Abstract

As a ceramic with high economic value, aluminum nitride possesses high thermal conductivity, excellent electrical insulation, high mechanical strength and high melting temperature and these all are required in high technologies involving cooling, insulation, thermal expansion and corrosion. This paper deals with thermodynamic parameters which affect the $\text{Al}_2\text{O}_3 \rightarrow \text{AlN}$ reduction efficiency during a carbothermal reduction. According to the carbothermal reduction reaction $\gamma\text{-Al}_2\text{O}_3 + 3\text{C} + \text{N}_2 \rightarrow \text{AlN} + 3\text{CO}$, if molar mixing ratio of $\gamma\text{-Al}_2\text{O}_3:\text{C} = 1:3$ at 1,601 °C or higher, the $\gamma\text{-Al}_2\text{O}_3$ can be reduced to AlN. This carbothermal reduction reaction is controlled by main parameters of carbon activity, and partial pressures of nitrogen, carbon monoxide and carbon dioxide. For example, if less carbon is added, a lower carbothermal reduction rate is resulted; however, if extra carbon is added, aluminum carbide (Al_4C_3) could be produced, or C could remain in AlN. Without $\text{N}_2(\text{g})$ added in the carbothermal reduction, $\text{Al}_2\text{O}_3(\gamma)$ may react with C to generate Al_4C_3 at a temperature higher than 2,250 °C. AlN prefers to form with a unity carbon activity, at a lower oxygen partial pressure, a higher carbon monoxide partial pressure, or at a higher temperature. In order to understand the relationship with N_2 , O_2 , CO , CO_2 , C, Al_2O_3 , AlN and Al_4C_3 , the Al-N-C-O system was investigated by thermodynamic calculations.

Keywords: AlN, Al_2O_3 , Carbothermal reaction, Ceramic, Phase transformation, Thermodynamics.

1. Introduction

Alumina stands for various aluminum oxide phases in the temperature range of 300~1200 °C, such as $\alpha\text{-Al}_2\text{O}_3$ (1,200 °C above), $\kappa\text{-Al}_2\text{O}_3$ (300~500 °C), $\eta\text{-Al}_2\text{O}_3$ (250~500 °C), $\gamma\text{-Al}_2\text{O}_3$ (500~850 °C), $\delta\text{-Al}_2\text{O}_3$ (850~1,050 °C) and $\theta\text{-Al}_2\text{O}_3$ (850~1,150 °C) (Boumaza et al., 2009). With stable chemical and insulating physical properties, the alumina especially $\alpha\text{-Al}_2\text{O}_3$ was used as a ceramic substrate which requires to be thermal conductive at a high temperature. Ceramic materials, for example, cubic boron nitride (*c*-BN), beryllium oxide (BeO) and aluminum nitride (AlN) have superior thermal conductivities and electrical insulating characteristics than alumina. Among these three compounds, though BeO and *c*-BN exhibit better thermal and electrical properties than AlN, use of toxic BeO is restricted in many applications, and it is difficult to produce *c*-BN. Currently, AlN has been widely used as a light-emitting diode (LED) substrate because of its excellent thermal conductivity, electrical insulation, and close match of thermal expansion with silicon.

Aluminum nitride, known as a ceramic material with high melting point (2,200 °C) and good chemical stability, is highly thermal conductive ($280 \text{ W m}^{-1}\text{K}^{-1}$) and electrical insulating (volume resistivity $>10^{14} \Omega\cdot\text{cm}$) (Xu et al., 2001). Its thermal conductivity is several times better than Al_2O_3 . So far, AlN powder has been fabricated by several methods. For example,

(1) Chemical method using $\text{Al}_2\text{O}_3 + \text{C}$ mixture, which is based on hydrolysis and precipitation by ammonia (NH_3) of an aluminium alkoxide in alcoholic suspension (Drauz et al.,

* Corresponding author: linjsh@ncut.edu.tw

1997);

(2) Sol-gel method, which includes steps of (a) mixing a boehmite (AlOOH) sol with a carbon source (carbon particles) material; (b) drying the mixture; (c) calcining in N-containing (and non-oxidizing) gas atmosphere; and (d) decarbonizing the obtained product (Chaudhuri et al., 2013);

(3) Carbothermal reduction, in which the production of AlN by thermal reduction of Al_2O_3 in a N_2 flow, with C/CH_4 as reducing agents ($\text{Al}_2\text{O}_3 + 3\text{C} + \text{N}_2 \rightarrow \text{AlN} + 3\text{CO}$) (Lefort et al., 1993; Contursi et al., 1991). In order to reduce the transformation temperature, there are several methods. For example, Qin et al. (2008) transformed amorphous alumina to $\gamma\text{-Al}_2\text{O}_3$, which was then directly nitrided to AlN at 1400 °C by carbothermal reduction with urea ($\text{CO}(\text{NH}_2)_2$) and glucose ($\text{C}_6\text{H}_{12}\text{O}_6 \cdot \text{H}_2\text{O}$) assistance. Someno et al. (1991) prepared AlN- Al_2O_3 composite films by microwave plasma chemical vapor deposition.

We have discussed phase equilibria in Ni-Al-O (Kuo et al., 2009) and Ti-Al-O (Chen, 2014) systems. In this work, we consider the equilibrium conditions in the Al-N-C-O system with variables of temperature, partial pressures of oxygen, nitrogen, carbon monoxide and carbon dioxide, activities of C between Al_2O_3 -AlN interface, and Gibbs free energy. The mechanisms of phase transformations in the Al-N-C-O system at high temperatures are thereby clarified. The purpose of the present work is to explain carbothermal reduction of $\text{Al}_2\text{O}_3 \rightarrow \text{AlN}$ by thermodynamic calculations, which provide guidelines to obtain the economic material, LED substrate of AlN.

2. Thermodynamic Calculations and Results

2.1. Phases in the Al-N-C-O System

The phase diagrams (Figure 1) of Al-C, Al-N and Al-O (Wriedt et al., 1985; SGTE, 2004a; SGTE, 2004b), and thermodynamic handbooks (Chase et al., 1985; Barin et al., 1989) have documented 9 different condensed phases and 8 gaseous phases in the Al-N-C-O system. The 17 phases are listed as follows: $\text{Al}(s, l)$, $\text{O}_2(g)$, $\text{Al}_2\text{O}_3(\alpha)$, $\text{Al}_2\text{O}_3(\kappa)$, $\text{Al}_2\text{O}_3(\delta)$, $\text{Al}_2\text{O}_3(\gamma)$, $\text{Al}_2\text{O}_3(\eta)$, $\text{Al}_2\text{O}_3(\theta)$, $\text{Al}(g)$, $\text{Al}_2\text{O}_2(g)$, $\text{Al}_2\text{O}(g)$, $\text{AlO}(g)$, $\text{Al}_2\text{O}_2(g)$, $\text{CO}(g)$, $\text{CO}_2(g)$, $\text{AlN}(s)$ and $\text{Al}_4\text{C}_3(s)$. Here, the subscripts of g and s represent gas and solid phases, respectively; and the other subscripts of α , κ , δ , γ , η and θ , the allotropy of Al_2O_3 . To simplify the calculation of phases in the Al-N-C-O system, the 5 gaseous species $\text{Al}(g)$, $\text{Al}_2\text{O}_2(g)$, $\text{Al}_2\text{O}(g)$, $\text{AlO}(g)$, and $\text{Al}_2\text{O}_2(g)$ with the exception of $\text{O}_2(g)$, $\text{N}_2(g)$, $\text{CO}(g)$ and $\text{CO}_2(g)$ are ignored at first because of their low partial vapor pressure within the Al-O system.

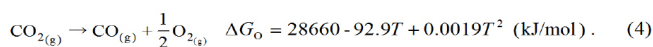
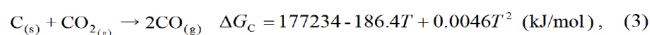
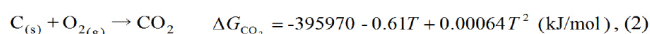
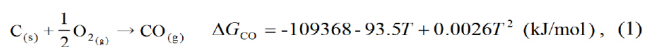
In the alumina phases of $\text{Al}_2\text{O}_3(\alpha)$, $\text{Al}_2\text{O}_3(\kappa)$, $\text{Al}_2\text{O}_3(\delta)$, $\text{Al}_2\text{O}_3(\gamma)$, $\text{Al}_2\text{O}_3(\eta)$ and $\text{Al}_2\text{O}_3(\theta)$, the $\text{Al}_2\text{O}_3(\gamma)$ is unstable as compared with other phases. Figure 2 shows the formation Gibbs free energy of $\text{Al}_2\text{O}_3(\gamma)$, $\text{Al}_2\text{O}_3(\delta)$, $\text{Al}_2\text{O}_3(\kappa)$ and $\text{Al}_2\text{O}_3(\alpha)$ at various temperatures. In Figure 2(a), the $\text{Al}_2\text{O}_3(\gamma)$ has the highest free energy value (unstable) while the $\text{Al}_2\text{O}_3(\alpha)$ has the lowest free energy value (stable). More clearly, Figure 2(b), (c) and (d) show the Gibbs free energy of alumina in the temperature ranges of 500-900 °C, 900-1,300 °C and 1,300-1,800 °C, respectively. Because $\text{Al}_2\text{O}_3(\gamma)$ is suitable to be converted to AlN

in the carbothermal reduction process, the $\text{Al}_2\text{O}_3(\alpha)$, $\text{Al}_2\text{O}_3(\kappa)$, $\text{Al}_2\text{O}_3(\delta)$, $\text{Al}_2\text{O}_3(\eta)$ and $\text{Al}_2\text{O}_3(\theta)$ are ignored in the thermodynamic calculation.

As a result, the Al-N-C-O system now only includes 4 condensed phases, i.e., $\text{Al}(s, l)$, $\text{Al}_2\text{O}_3(\gamma)$, $\text{AlN}(s)$ and $\text{Al}_4\text{C}_3(s)$, and 4 gas phases of $\text{O}_2(g)$, $\text{N}_2(g)$, $\text{CO}(g)$ and $\text{CO}_2(g)$. The 5 basic Al-N-C-O system reaction equations are in the Table 1. The thermodynamic stabilities of compounds in the Al-N-C-O system were evaluated by considering their Gibbs free energy, based on the data in Table 1. In the Al-N-C-O, in an ascending order of Gibbs free energy, the compounds below 827 K are $\text{Al}_2\text{O}_3(\gamma) \rightarrow \text{CO}_2(g) \rightarrow \text{AlN}(s) \rightarrow \text{CO}(g) \rightarrow \text{Al}_4\text{C}_3(s)$. When the temperature is higher than 827 K, the ascending order becomes $\text{Al}_2\text{O}_3(\gamma) \rightarrow \text{CO}_2(g) \rightarrow \text{CO}(g) \rightarrow \text{AlN}(s) \rightarrow \text{Al}_4\text{C}_3(s)$ (Figure 3). Thus, $\text{Al}_2\text{O}_3(\gamma)$ is the most stable phase, and $\text{Al}_4\text{C}_3(s)$ is the least stable compound. Figure 3 also shows the formation Gibbs free energy of all compounds Al_2O_3 , CO_2 , CO , AlN , Al_4C_3 and Al_2O_3 . It is impossible to decompose the compounds without controlling the reduction conditions, for example, oxygen pressure and carbon activity.

2.2. C-O System

In carbothermal reduction, the reaction gases are carbon, oxygen, carbon monoxide and carbon dioxide. Here we discuss the relationship in the C(g), $\text{O}_2(g)$, $\text{CO}(g)$ and $\text{CO}_2(g)$ at high temperature reaction. In C-O system, the following reactions can be denoted: (a) C reacts with $\text{O}_2(g)$ to form $\text{CO}(g)$; (b) C reacts with $\text{O}_2(g)$ to form $\text{CO}_2(g)$; (c) C reacts with $\text{CO}_2(g)$ to form $\text{CO}(g)$; and (d) $\text{CO}_2(g)$ decompose to $\text{CO}(g)$ and $\text{O}_2(g)$. The reaction equations and the formation Gibbs free energy (Chase et al., 1985; Barin et al., 1989) are shown as:



The equilibrium partial vapor pressures of $\text{O}_2(g)$, $\text{CO}(g)$ and $\text{CO}_2(g)$ in C-O system can be calculated from the Gibbs free energy as follows, for example, the ΔG_{CO} is given by

$$\Delta G_{\text{CO}} = -RT \ln K_{\text{CO}}, \text{ or} \quad (5)$$

$$\log K_{\text{CO}} = \frac{-\Delta G_{\text{CO}}}{2.303RT}. \quad (6)$$

Here, K_{CO} , K_{CO_2} , K_{C} and K_{O} can be expressed as:

$$K_{\text{CO}} = \frac{P_{\text{CO}}}{a_{\text{C}}(P_{\text{O}_2})^{0.5}}, \quad (7)$$

$$K_{\text{CO}_2} = \frac{P_{\text{CO}_2}}{a_{\text{C}}P_{\text{O}_2}}, \quad (8)$$

$$K_{\text{C}} = \frac{(P_{\text{CO}})^2}{a_{\text{C}}P_{\text{CO}_2}}, \quad (9)$$

$$K_{\text{O}_2} = \frac{P_{\text{CO}}(P_{\text{O}_2})^{0.5}}{P_{\text{CO}_2}}, \quad (10)$$

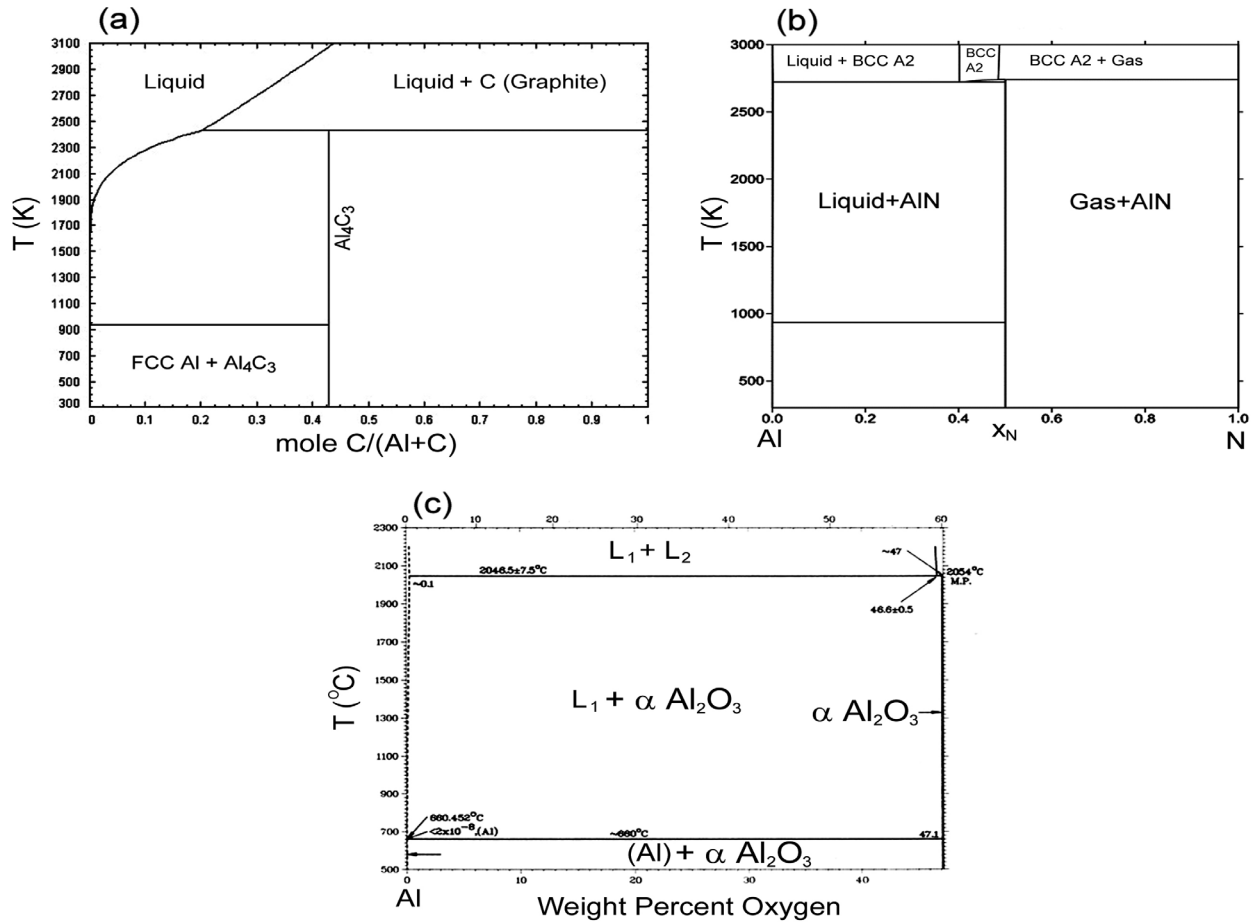


Figure 1. (a) Al-C phase diagram; (b) Al-N phase diagram; (c) Al-O phase diagram.

Here a_c , P_{CO} , P_{CO_2} , P_{O_2} , R , and T represent the activity of C, partial pressure of CO, CO₂, and O₂, gas constant, temperature (K), respectively. In Eqn. 6, K and R are constants; therefore, ΔG is only a function of temperature T . The ΔG can be expressed as $\Delta G = A + BT$, where A and B are two numerical numbers.

In order to precisely describe the C-O curves, the $\Delta G = A + BT$ is presented by quadratic equation of $\Delta G = A + BT + CT^2$. Therefore, $\log K_{CO}$, $\log K_{CO_2}$, $\log K_C$, and $\log K_O$ can be represented as:

$$\log K_{CO} = \frac{5712.03}{T} + 4.8852 - 0.0001362 T, \quad (11)$$

$$\log K_{CO_2} = \frac{20680.529}{T} + 0.0319 - 0.0000335 T, \quad (12)$$

$$\log K_C = \frac{-9256.469}{T} + 9.7385 - 0.0002389 T, \quad (13)$$

$$\log K_O = \frac{14968.499}{T} + 4.8533 - 0.0001027 T. \quad (14)$$

Here, we define R and P_t as:

$$R = \frac{P_{CO}}{P_{CO_2}}, \quad (15)$$

$$P_t = P_{CO} + P_{CO_2}. \quad (16)$$

It is assumed that carbon activity is unity ($a_c = 1$) and a lower

oxygen pressure in the carbothermal reduction, the relationship between R and P_{O_2} is presented as:

$$R = \frac{P_{CO}}{P_{CO_2}} = \frac{K_{CO} \times a_c \times P_{O_2}^{\frac{1}{2}}}{K_{CO_2} \times a_c \times P_{O_2}} = \frac{K_{CO}}{K_{CO_2}} \times P_{O_2}^{-\frac{1}{2}} \\ = 10^{\left(-\frac{14968.5}{T} + 4.8533 - 0.0001027 T\right)} \times P_{O_2}^{\frac{1}{2}}. \quad (17)$$

Based on the Eqn. 6, Figure 4 shows the curve with respect to $\log R$ and T . The figure presents the CO(g) and CO₂(g) characteristics at various temperature and oxygen pressure. A higher temperature results in a higher R value, which means CO(g) is stable than CO₂(g) at a higher temperature. Based on the Eqn. 17, the carbon activity is

$$a_c = \frac{R^2 \times P_t}{K_C(R+1)}. \quad (18)$$

In Figure 5, it is evident that R value increases either with carbon activity or temperature. From the above results, it is concluded that a lower O₂ partial pressure, a higher C activity, a higher CO partial pressure, or a lower CO₂ partial pressure enhances to achieve a higher carbothermal reduction efficiency.

Table 1. Five basic reaction equations in Al-N-C-O system.

No.	Reaction	$\log K$	ΔG (kJ/mol)
1	$2\text{Al}_{(s,l)} + \frac{3}{2}\text{O}_{2(g)} \rightarrow \text{Al}_2\text{O}_{3(\gamma)}$	$\log K_{\text{Al}_2\text{O}_3(\gamma)} = -16.61 + \frac{86886}{T}$	$\Delta G_{\text{Al}_2\text{O}_3(\gamma)} = -1663.26 + 0.328T$
2	$\text{C}_{(s)} + \frac{1}{2}\text{O}_{2(g)} \rightarrow \text{CO}_{(g)}$	$\log K_{\text{CO}} = 4.48 + \frac{6004}{T}$	$\Delta G_{\text{CO}} = -114.97 - 0.086T$
3	$\text{C}_{(s)} + \text{O}_{2(g)} \rightarrow \text{CO}_{2(g)}$	$\log K_{\text{CO}_2} = -0.01 + \frac{20702}{T}$	$\Delta G_{\text{CO}_2} = -396.38 + 0.0001T$
4	$\text{Al}_{(s,l)} + \frac{1}{2}\text{N}_{2(g)} \rightarrow \text{AlN}_{(s)}$	$\log K_{\text{AlN}} = -6.13 + \frac{17193}{T}$	$\Delta G_{\text{AlN}} = -329.21 + 0.117T$
5	$4\text{Al}_{(s,l)} + 3\text{C}_{(s)} \rightarrow \text{Al}_4\text{C}_{3(s)}$	$\log K_{\text{Al}_4\text{C}_3} = -5.07 + \frac{13935}{T}$	$\Delta G_{\text{Al}_4\text{C}_3} = -266.84 + 0.097T$

Table 2. Four various reaction equations in Al-N-C-O system.

No.	Reaction	$\log K$ and ΔG (kJ/mol)
1	$\text{Al}_2\text{O}_{3(\gamma)} + 3\text{C}_{(s)} + \text{N}_{2(g)} \rightarrow 2\text{AlN}_{(s)} + 3\text{CO}_{(g)} ;$ $\log P_{\text{CO}} = \frac{1}{3}(\log K_1 + 3\log a_c + \log P_{\text{N}_2})$	$\log K_1 = 17.79 - \frac{34488}{T} ;$ $\Delta G_1 = 659.93 - 0.35T$ $T = 1874 \text{ K}; \Delta G_1 = 0$
2	$2\text{Al}_2\text{O}_{3(\gamma)} + 3\text{C} \rightarrow \text{Al}_4\text{C}_{3(s)} + 3\text{O}_{2(g)} ;$ $\log P_{\text{O}_2} = \frac{1}{3}(\log K_2 + 3\log a_c)$	$\log K_2 = 28.15 - \frac{159837}{T} ;$ $\Delta G_2 = 3060.40 - 0.54T$ $T = 5667 \text{ K}; \Delta G_2 = 0$
3	$\text{Al}_2\text{O}_{3(\gamma)} + \text{N}_{2(g)} \rightarrow 2\text{AlN}_{(s)} + \frac{3}{2}\text{O}_{2(g)} ;$ $\log P_{\text{O}_2} = \frac{2}{3}(\log K_3 + \log P_{\text{N}_2})$	$\log K_3 = 4.35 - \frac{52500}{T} ;$ $\Delta G_3 = 1005.22 - 0.08T$ $T = 12562 \text{ K}; \Delta G_3 = 0$
4	$3\text{Al}_2\text{O}_{3(\gamma)} + 6\text{C}_{(s)} + \text{N}_{2(g)} \rightarrow 2\text{AlN}_{(s)} + 3\text{CO}_{(g)} + \text{Al}_4\text{C}_{3(s)} + 3\text{O}_{2(g)}$ $\log P_{\text{O}_2} = \frac{1}{3}(\log K_4 + \log P_{\text{N}_2} - \log P_{\text{CO}})$	$\log K_4 = 45.94 - \frac{194325}{T} ;$ $\Delta G_4 = 3720.74 - 0.88T$ $T = 4227 \text{ K}; \Delta G_4 = 0$

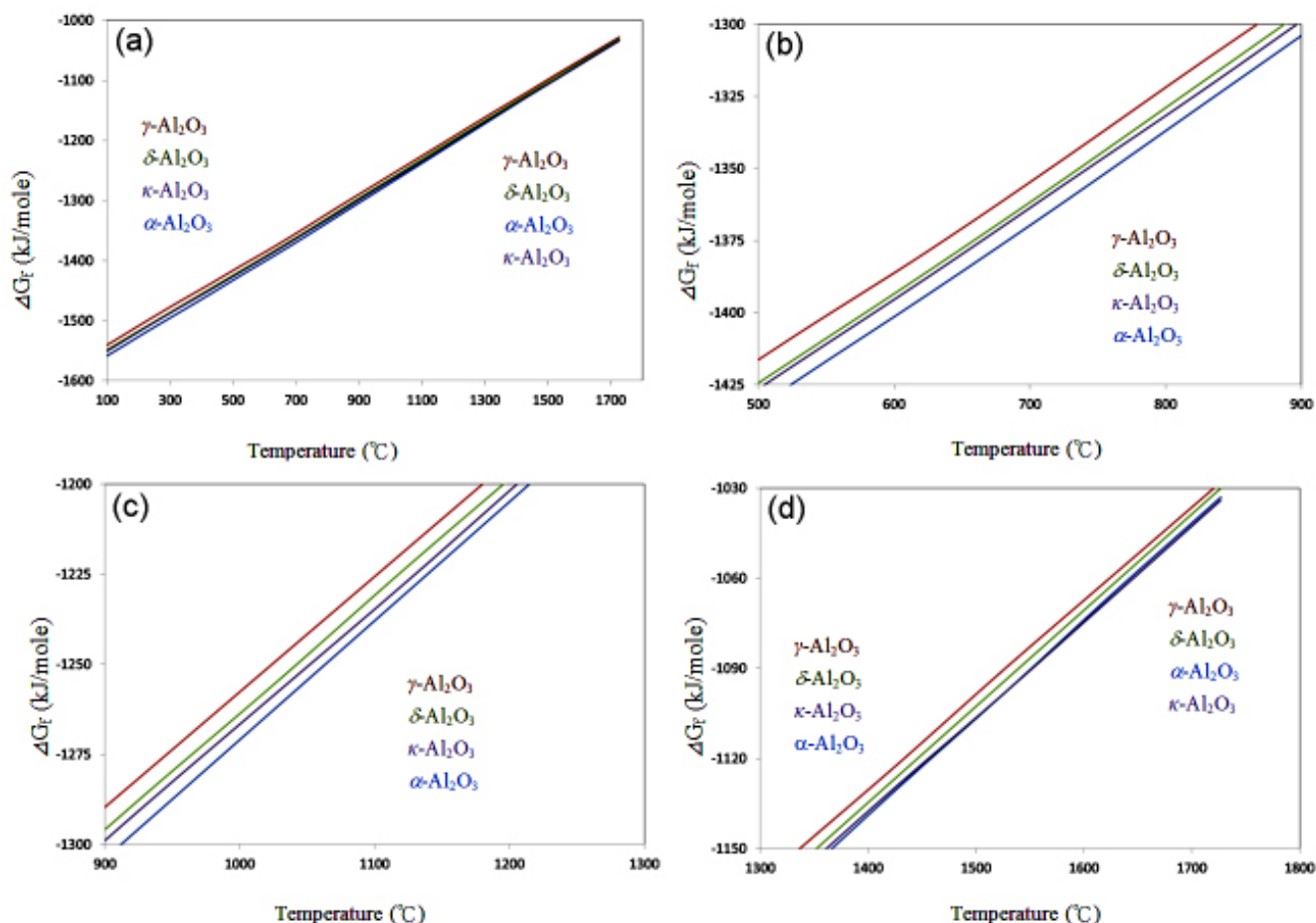


Figure 2. Thermodynamic stability characteristics of various Al_2O_3 in the ΔG - T diagram. γ - Al_2O_3 is unstable as compared with δ - Al_2O_3 , κ - Al_2O_3 , and α - Al_2O_3 .

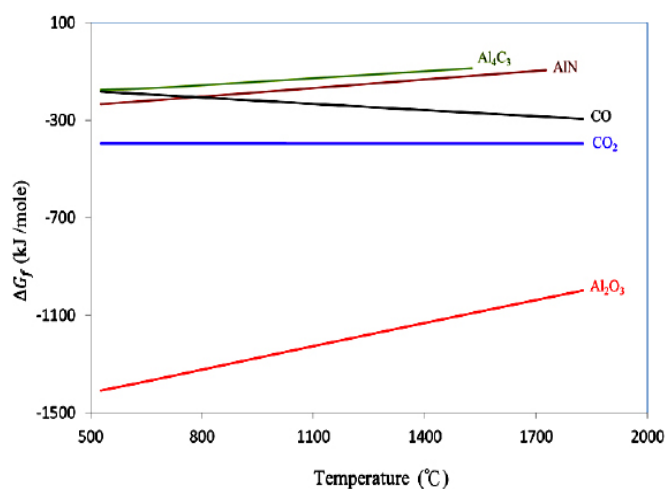


Figure 3. Thermodynamic stability characteristics of various Al_2O_3 , CO_2 , CO , AlN , and Al_4C_3 in the ΔG - T diagram. Al_2O_3 is the most stable compound compares to the CO_2 , CO , AlN , and Al_4C_3 compounds.

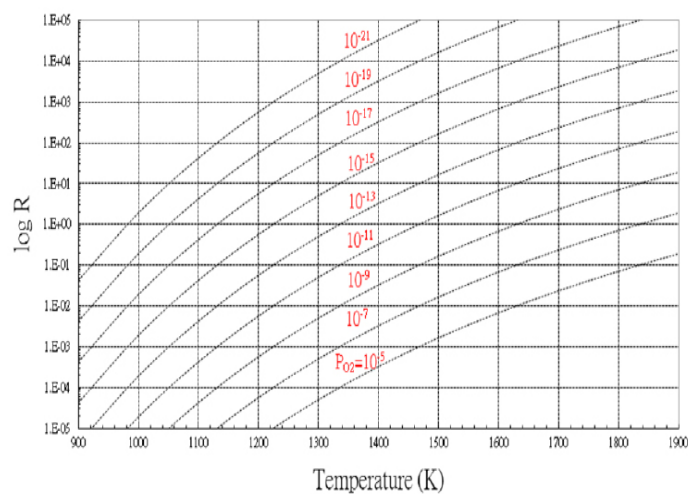


Figure 4. Oxygen partial pressure P_{O_2} at $\log R$ and T .

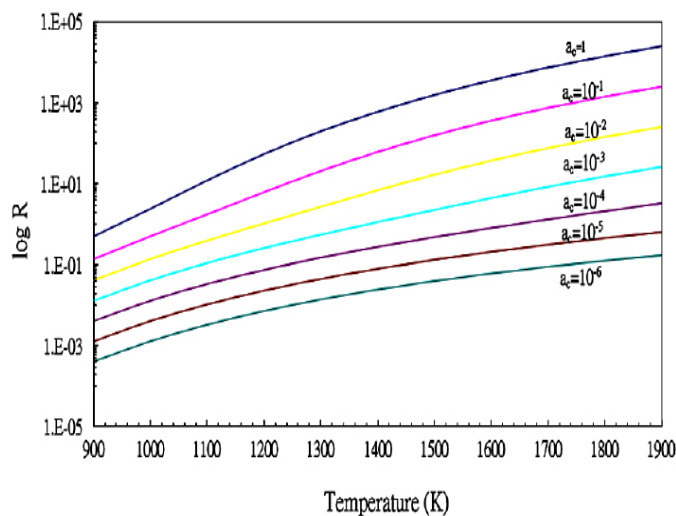


Figure 5. Carbon activity P_{O_2} at $\log R$ and T .

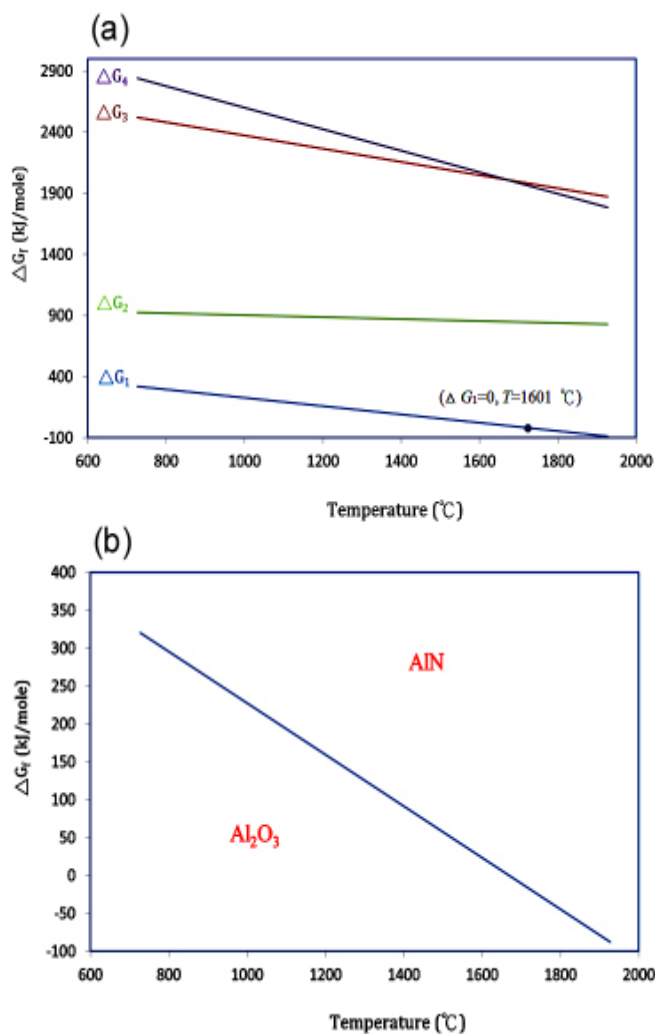


Figure 6. (a) Compounds formation Gibbs free energy curves in the temperature range from 700 to 1,900 °C; (b) stable $Al_2O_3(\gamma)$ and stable $AlN(s)$ regions.

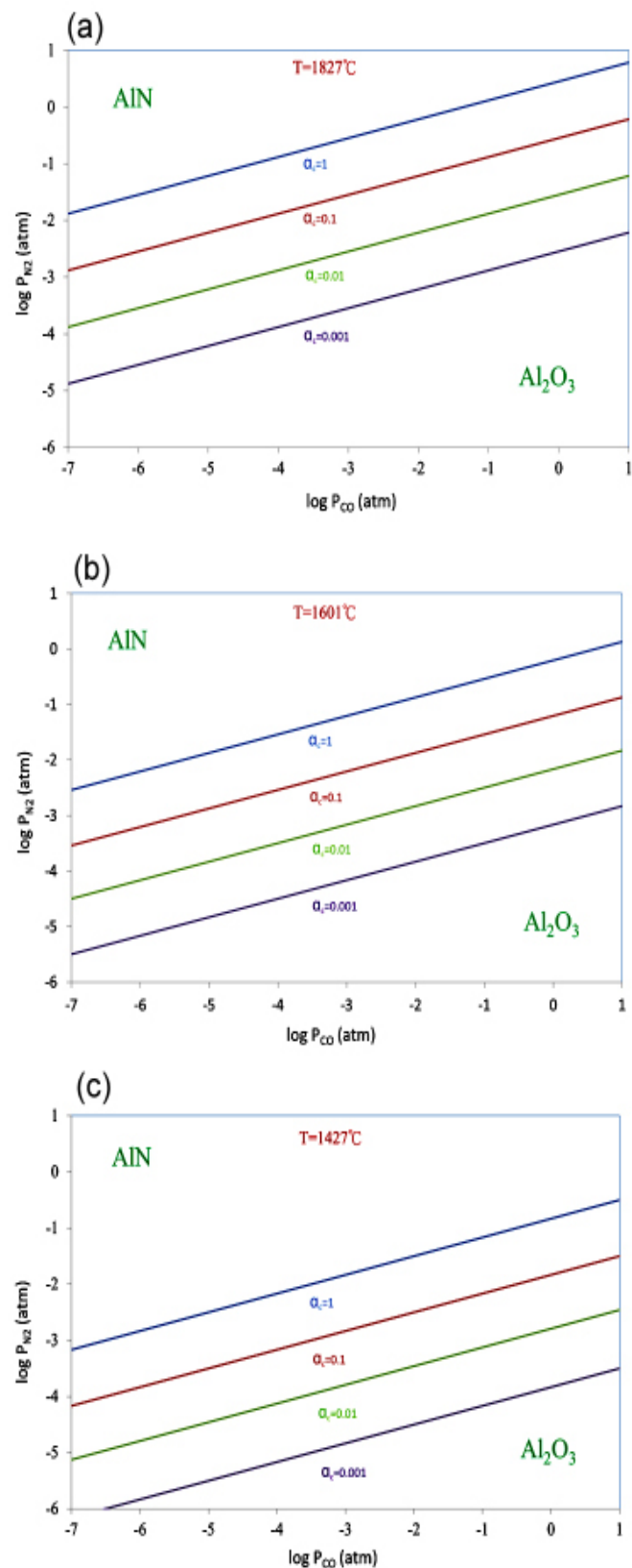
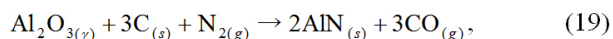


Figure 7. Stable regions of AlN and Al_2O_3 when the reaction temperature is higher than the carbothermal reduction at 1,827 °C (a), at carbothermal reduction at 1,601 °C (b), or below than the carbothermal reduction at 1,427 °C (c).

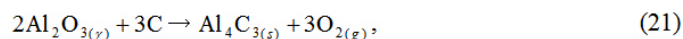
2.3. Al-N-C-O System

Carbothermal reduction is usually used to achieve the $\text{Al}_2\text{O}_3 \rightarrow \text{AlN}$ transformation. The carbothermal reduction is a solid-solid reaction between alumina and carbon powders in a nitrogen atmosphere. In order to obtain a lower transformation temperature during $\text{Al}_2\text{O}_3(\gamma) \rightarrow \text{AlN}(s)$ by carbothermal reduction method, the $\text{Al}_2\text{O}_3(\gamma)$ usually reacts with $\text{N}_2(g)$ and $\text{C}(s)$ under a lower oxygen pressure chamber. The reaction equation and Gibbs free energy of $\text{Al}_2\text{O}_3(\gamma)$ to $\text{AlN}(s)$ by carbothermal reduction are presented as follows:

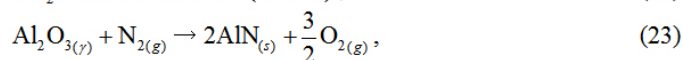


$$\Delta G_1 = 659.93 - 0.35T \text{ (kJ/mol)}. \quad (20)$$

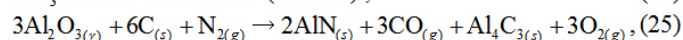
In Eqn. 19, the conversion step from $\text{Al}_2\text{O}_3(\gamma)$ to $\text{AlN}(s)$ by carbothermal reduction includes decomposition of $\text{Al}_2\text{O}_3(\gamma)$ (positive free energy), formation of CO gas (negative free energy), and formation $\text{AlN}(s)$ compound (negative free energy). The net free energy in Eqn. 20 is zero at 1,601 °C. Therefore, the equilibrium temperature is 1,874 K (1,601 °C), which means to convert $\text{Al}_2\text{O}_3(\gamma)$ to $\text{AlN}(s)$ by the carbothermal reduction, the reaction temperature must be higher than 1874 K. If no $\text{N}_2(g)$ is involved in the carbothermal reduction, the $\text{Al}_2\text{O}_3(\gamma)$ may react with C, yielding reduction of Al at a temperature higher than 2,250 °C, or formation of $\text{Al}_4\text{C}_3(s)$. The reaction equation and Gibbs free energy of $\text{Al}_2\text{O}_3(\gamma) \rightarrow \text{Al}$ and $\text{Al}_2\text{O}_3(\gamma) \rightarrow \text{Al}_4\text{C}_3(s)$ by carbothermal reductions are presented in Eqns. 21 and 22, respectively. In Eqn. 22, when $\Delta G_2 = 0$, the equilibrium temperature is 5,667 K (5,394 °C), which means to convert $\text{Al}_2\text{O}_3(\gamma)$ to $\text{Al}_4\text{C}_3(s)$ by the carbothermal reduction, the reaction temperature must be higher than 5,667 K. Moreover, Eqns. 23 and 24 represent the reaction equation and Gibbs free energy of $\text{Al}_2\text{O}_3(\gamma) \rightarrow \text{AlN}(s)$ by thermo-nitrogen reduction, respectively. The reaction temperature must be higher than 12,562 K (12,289 °C). According to Eqns. 25 and 26, if $\text{Al}_2\text{O}_3(\gamma)$ reacts with extra C to be converted to $\text{AlN}(s)$ and $\text{Al}_4\text{C}_3(s)$ by the carbothermal reduction, the temperature must be higher than 4,277 K (4,004 °C). The thermodynamic reaction equations to convert $\text{Al}_2\text{O}_3(\gamma)$ to $\text{AlN}(s)$ and $\text{Al}_4\text{C}_3(s)$ are summarized in the Table 2. Figure 6(a) shows the free energy curves in the temperature range from 700 to 1,900 °C. From the free energy curve, when $\text{Al}_2\text{O}_3(\gamma):\text{C} = 1:3$ in mole, ΔG_1 is negative if the temperature is above 1,601 °C. However, the free energy curves of ΔG_2 , ΔG_3 , and ΔG_4 are all positive. In Figure 6(b), the ΔG_1 curve separates stable $\text{Al}_2\text{O}_3(\gamma)$ and stable $\text{AlN}(s)$ regions.



$$\Delta G_2 = 3060.40 - 0.54T \text{ (kJ/mol)}; \quad (22)$$



$$\Delta G_3 = 1005.22 - 0.08T \text{ (kJ/mol)}; \quad (24)$$



$$\Delta G_4 = 3720.74 - 0.88T \text{ (kJ/mol)}. \quad (26)$$

Figure 7 shows the stable regions of AlN and Al_2O_3 , which are controlled by the carbon activity, oxygen partial pressure, nitrogen partial pressure and temperature. When the partial

pressure of CO is fixed, the partial pressure of N_2 increases with carbon activity and temperature. Because the AlN quantity is directly proportional to the N_2 partial pressure, AlN prefers to form in a higher carbon activity or a higher reaction temperature. The two regions are shown in Figure 7(a) when the reaction temperature is higher than the carbothermal reduction of 1,827 °C, Figure 7(b) when the temperature is at 1,601 °C, and Figure 7(c) when the temperature is below the carbothermal reduction at 1,427 °C. Higher reaction temperature and carbon activity will yield higher N_2 pressure. For example, when $P_{\text{CO}} = 10^{-3}$ atm and carbon activity $a_{\text{C}}=1$, the N_2 pressures are $10^{-1.83}$ atm, $10^{-1.20}$ atm, and $10^{-0.54}$ atm at 1,427 °C, 1,601 °C and 1,827 °C, respectively.

3. Conclusions

Thermodynamic calculations were conducted to estimate $\text{Al}_2\text{O}_3 \rightarrow \text{AlN}$ transformation under various partial oxygen, nitrogen, carbon monoxide, carbon dioxide pressures and the activities of carbon in the Al-N-C-O system. According to the thermodynamic calculations, a lower oxygen pressure, a higher nitrogen pressure, a higher carbon activity, or a higher temperature promotes to the $\text{Al}_2\text{O}_3(\gamma) \rightarrow \text{AlN}$ transformation in the carbothermal reduction process. The idea molar mixing ratio of $\gamma\text{-Al}_2\text{O}_3:\text{C}$ is 1:3; however, in reality it is difficult to cover $\gamma\text{-Al}_2\text{O}_3$ particles with carbon particles uniformly. The carbothermal reduction temperature is usually higher than the theoretical temperature of 1,601 °C.

The following findings are obtained:

(1) The carbothermal reduction is a solid-solid reaction between alumina and carbon powders in a nitrogen atmosphere. If insufficient quantity of carbon is added, the carbothermal reduction rate decreases; however, if extra carbon is added, aluminum carbide (Al_4C_3) may appear or C may remain in AlN .

(2) If the molar mixing ratio of $\gamma\text{-Al}_2\text{O}_3:\text{C} = 1:3$ at 1,601 °C or higher, the $\gamma\text{-Al}_2\text{O}_3$ may be reduced to AlN .

(3) The stability region of AlN and Al_2O_3 are controlled by the carbon activity, oxygen partial pressure, nitrogen partial pressure and temperature. In the carbon reduction of $\text{Al}_2\text{O}_3 \rightarrow \text{AlN}$ when $P_{\text{CO}} = 10^{-3}$ atm and carbon activity is 1, $P_{\text{N}_2} = 10^{-1.20}$ atm at 1,601 °C.

Acknowledgements

This work was financially supported by the Chung-Shan Institute of Science and Technology (CSIST), Taiwan, under the contract No. XD03034P.

References

- Barin I (1989), Thermochemical Data of Pure Substances. VCH verlagsgesellschaft mbh, New York, USA, pp.42, 44-51, 271-272.
- Boumaza A, L Favaro, J Lédion, G Sattonnay, JB Brubach, and AM Huntz (2009) Transition Alumina Phases Induced by Heat Treatment of Boehmite: An X-ray Diffraction and Infrared Spectroscopy Study. Journal of Solid State Chemistry 182 (5): 1171-1176.
- Chase MW, Jr. CA Davies, JR Downey, Jr. DJ Furip, RA McDonald,

- and AN Syverud (1985) JANAF Thermochemical Tables Third Edition. American Chemical Society, New York, USA, p.p. 131, 152-161, 626, 628, 672.
- Chaudhuri MG, J Bas, GC Das, S Mukherjee, and MK Mitra (2013) A Novel Method of Synthesis of Nanostructured Aluminum Nitride Through Sol-Gel Route by In Situ Generation of Nitrogen. Journal of the American Ceramic Society 96 (2): 385–390.
- Chen CC (2014) Phase Equilibria at Ti–Al Interface under Low Oxygen Pressure Atlas Journal of Materials Science 1(1):1-11.
- Contursi GB and G Beghelli (1991) Process for Preparing Fine Aluminum Nitride Powder From an Inorganic Flocculant. US patent: US5219539 A.
- Drauz K, T Muller, and M Kottenhahn, D Seebach, A Thaler (1997) Transesterification and Other Conversion Reactions of Acid Derivatives using an Amidine. US patent US 6090913 A.
- Kuo CG, WD Jehng, SJ Hsieh, and CC Chen (2009) Phase Equilibria on Ni–Al Interface Under Low Oxygen Pressure, J. Alloys Compd. 480 (2): 299-305.
- Lefort P, and M Billy (1993) Mechanism of AlN Formation through the Carbothermal Reduction of Al₂O₃ in a Flowing N₂ Atmosphere. Journal of the American Ceramic Society 76 (9): 2295-2299.
- Qin M, X Du, Z Li, IS Humail, and X Qu (2008) Synthesis of Aluminum Nitride Powder by Carbothermal Reduction of a Combustion Synthesis Precursor. Materials Research Bulletin 43 (11): 2954-2960.
- SGTE alloy databases (2004a) Al-C binary phase diagram. http://www.crct.polymtl.ca/fact/phase_diagram.php?file=Al-C.jpg&dir=SGTE
- SGTE alloy databases (2004b) Al-N binary phase diagram. http://www.crct.polymtl.ca/fact/phase_diagram.php?file=Al-N.jpg&dir=SGTE
- Somono Y, M Sasaki, and T Hirai (1991) Preparation of AlN-Al₂O₃ Composite Films by Microwave Plasma Chemical Vapor Deposition. Japanese Journal of Applied Physics 30 (8): 1792-1797.
- Wriedt HA (1985) The Al-O (Aluminum-Oxygen) System. Bulletin of Alloy Phase Diagrams 6 (6): 548-553.
- Xu Y, DDL Chung, and C Mroz (2001) Thermally Conducting Aluminum Nitride Polymer-Matrix Composites. Composites: Part A 32 (12): 1749-1757.